Study of the process $e^+e^- \to \phi\eta$ at center-of-mass energies between 2.00 and 3.08 GeV

M. Ablikim,[1] M. N. Achasov,[10,b] P. Adlarson,[67] S. Ahmed,[15] M. Albrecht,[4] R. Aliberti,[28] A. Amoroso,[66a,66c] M. R. An,[32] Q. An,[63,49] X. H. Bai,[57] Y. Bai,[48] O. Bakina,[29] R. Baldini Ferroli,[23a] I. Balossino,[24a] Y. Ban,[38,h] K. Begzsuren,[26] N. Berger,[28] M. Bertani,[23a] D. Bettoni,[24a] F. Bianchi,[66a,66c] J. Bloms,[60] A. Bortone,[66a,66c] I. Boyko,[29] R. A. Briere,[5] H. Cai,[68] X. Cai,[1,49] A. Calcaterra,[23a] G. F. Cao,[1,54] N. Cao,[1,54] S. A. Cetin,[53a] J. F. Chang,[1,49] W. L. Chang,[1,54] G. Chelkov,[29,a] D. Y. Chen,[6] G. Chen,[1] H. S. Chen,[1,54] M. L. Chen,[1,49] S. J. Chen,[35] X. R. Chen,[25] Y. B. Chen,[1,49] Z. J. Chen,[20,i] W. S. Cheng,[66c] G. Cibinetto,[24a] F. Cossio,[66c] X. F. Cui,[36] H. L. Dai,[1,49] X. C. Dai,[1,54] A. Dbeyssi,[15] R. E. de Boer,[4] D. Dedovich,[29] Z. Y. Deng,[1] A. Denig,[28] I. Denysenko,[29] M. Destefanis,[66a,66c] F. De Mori,[66a,66c] Y. Ding,[33] C. Dong,[36] J. Dong,[1,49] L. Y. Dong,[1,54] M. Y. Dong,[1,49,54] X. Dong,[68] S. X. Du,[71] Y. L. Fan,[68] J. Fang,[1,49] S. S. Fang,[1,54] Y. Fang,[1] R. Farinelli,[24a] L. Fava,[66b,66c] F. Feldbauer,[4] G. Felici,[23a] C. Q. Feng,[63,49] J. H. Feng,[50] M. Fritsch,[4] C. D. Fu,[1] X. L. Gao,[63,49] Y. Gao,[38,h] Y. Gao,[64] Y. Gao,[63,49] Y. G. Gao,[6] I. Garzia,[24a,24b] P. T. Ge,[68] C. Geng,[50] E. M. Gersabeck,[58] A. Gilman,[61] K. Goetzen,[11] L. Gong,[33] W. X. Gong,[1,49] W. Gradl,[28] M. Greco,[66a,66c] L. M. Gu,[35] M. H. Gu,[1,49] Y. T. Gu,[13] C. Y. Guan,[1,54] A. Q. Guo,[22] L. B. Guo,[34] R. P. Guo,[40] Y. P. Guo,[9,f] A. Guskov,[29,a] T. T. Han,[41] W. Y. Han,[32] X. Q. Hao,[16] F. A. Harris,[56] K. L. He,[1,54] F. H. Heinsius,[4] C. H. Heinz,[28] T. Held,[4] Y. K. Heng,[1,49,54] C. Herold,[51] M. Himmelreich,[11,d] T. Holtmann,[4] G. Y. Hou,[1,54] Y. R. Hou,[54] Z. L. Hou,[1] H. M. Hu,[1,54] J. F. Hu,[47,j] T. Hu,[1,49,54] Y. Hu,[1] G. S. Huang,[63,49] L. Q. Huang,[64] X. T. Huang,[41] Y. P. Huang,[1] Z. Huang,[38,h] T. Hussain,[65] N. Hüsken,[22,28] W. Ikegami Andersson,[67] W. Imoehl,[22] M. Irshad,[63,49] S. Jaeger,[4] S. Janchiv,[26] Q. Ji,[1] Q. P. Ji,[16] X. B. Ji,[1,54] X. L. Ji,[1,49] Y. Y. Ji,[41] H. B. Jiang,[41] X. S. Jiang,[1,49,54] J. B. Jiao,[41] Z. Jiao,[18] S. Jin,[35] Y. Jin,[57] M. Q. Jing,[1,54] T. Johansson,[67] N. Kalantar-Nayestanaki,[55] X. S. Kang,[33] R. Kappert,[55] M. Kavatsyuk,[55] B. C. Ke,[43,1] I. K. Keshk,[4] A. Khoukaz,[60] P. Kiese,[28] R. Kiuchi,[1] R. Kliemt,[11] L. Koch,[30] O. B. Kolcu,[53a,m] B. Kopf,[4] M. Kuemmel,[4] M. Kuessner,[4] A. Kupsc,[67] M. G. Kurth,[1,54] W. Kühn,[30] J. J. Lane,[58] J. S. Lange,[30] P. Larin,[15] A. Lavania,[21] L. Lavezzi,[66a,66c] Z. H. Lei,[63,49] H. Leithoff,[28] M. Lellmann,[28] T. Lenz,[28] C. Li,[39] C. H. Li,[32] Cheng Li,[63,49] D. M. Li,[71] F. Li,[1,49] G. Li,[1] H. Li,[43] H. Li,[63,49] H. B. Li,[1,54] H. J. Li,[16] J. L. Li,[41] J. Q. Li,[4] J. S. Li,[50] Ke Li,[1] L. K. Li,[1] Lei Li,[3] P. R. Li,[31,k,l] S. Y. Li,[52] W. D. Li,[1,54] W. G. Li,[1] X. H. Li,[63,49] X. L. Li,[41] Xiaoyu Li,[1,54] Z. Y. Li,[50] H. Liang,[63,49] H. Liang,[1,54] H. Liang,[27] Y. F. Liang,[45] Y. T. Liang,[25] G. R. Liao,[12] L. Z. Liao,[1,54] J. Libby,[21] C. X. Lin,[50] B. J. Liu,[1] C. X. Liu,[1] D. Liu,[15,63] F. H. Liu,[44] Fang Liu,[1] Feng Liu,[6] H. B. Liu,[13] H. M. Liu,[1,54] Huanhuan Liu,[1] Huihui Liu,[17] J. B. Liu,[63,49] J. L. Liu,[64] J. Y. Liu,[1,54] K. Liu,[1] K. Y. Liu,[33] L. Liu,[63,49] M. H. Liu,[9,f] P. L. Liu,[1] Q. Liu,[54] Q. Liu,[68] S. B. Liu,[63,49] Shuai Liu,[46] T. Liu,[1,54] W. M. Liu,[63,49] X. Liu,[31,k,l] Y. Liu,[31,k,l] Y. B. Liu,[36] Z. A. Liu,[1,49,54] Z. Q. Liu,[41] X. C. Lou,[1,49,54] F. X. Lu,[50] H. J. Lu,[18] J. D. Lu,[1,54] J. G. Lu,[1,49] X. L. Lu,[1] Y. Lu,[1] Y. P. Lu,[1,49] C. L. Luo,[34] M. X. Luo,[70] P. W. Luo,[50] T. Luo,[9,f] X. L. Luo,[1,49] X. R. Lyu,[54] F. C. Ma,[33] H. L. Ma,[1] L. L. Ma,[41] M. M. Ma,[1,54] Q. M. Ma,[1] R. Q. Ma,[1,54] R. T. Ma,[54] X. X. Ma,[1,54] X. Y. Ma,[1,49] F. E. Maas,[15] M. Maggiora,[66a,66c] S. Maldaner,[4] S. Malde,[61] Q. A. Malik,[65] A. Mangoni,[23b] Y. J. Mao,[38,h] Z. P. Mao,[1] S. Marcello,[66a,66c] Z. X. Meng,[57] J. G. Messchendorp,[55] G. Mezzadri,[24a] T. J. Min,[35] R. E. Mitchell,[22] X. H. Mo,[1,49,54] Y. J. Mo,[6] N. Yu. Muchnoi,[10,b] H. Muramatsu,[59] S. Nakhoul,[11,d] Y. Nefedov,[29] F. Nerling,[11,d] I. B. Nikolaev,[10,b] Z. Ning,[1,49] S. Nisar,[8,g] Q. Ouyang,[1,49,54] S. Pacetti,[23b,23c] X. Pan,[9,f] Y. Pan,[58] A. Pathak,[1] A. Pathak,[27] P. Patteri,[23a] M. Pelizaeus,[4] H. P. Peng,[63,49] K. Peters,[11,d] J. Pettersson,[67] J. L. Ping,[34] R. G. Ping,[1,54] S. Pogodin,[29] R. Poling,[59] V. Prasad,[63,49] H. Qi,[63,49] H. R. Qi,[52] K. H. Qi,[25] M. Qi,[35] T. Y. Qi,[9] S. Qian,[1,49] W. B. Qian,[54] Z. Qian,[50] C. F. Qiao,[54] L. Q. Qin,[12] X. P. Qin,[9] X. S. Qin,[41] Z. H. Qin,[1,49] J. F. Qiu,[1] S. Q. Qu,[36] K. H. Rashid,[65] K. Ravindran,[21] C. F. Redmer,[28] A. Rivetti,[66c] V. Rodin,[55] M. Rolo,[66c] G. Rong,[1,54] Ch. Rosner,[15] M. Rump,[60] H. S. Sang,[63] A. Sarantsev,[29,c] Y. Schelhaas,[28] C. Schnier,[4] K. Schoenning,[67] M. Scodeggio,[24a,24b] D. C. Shan,[46] W. Shan,[19] X. Y. Shan,[63,49] J. F. Shangguan,[46] M. Shao,[63,49] C. P. Shen,[9] H. F. Shen,[1,54] P. X. Shen,[36] X. Y. Shen,[1,54] H. C. Shi,[63,49] R. S. Shi,[1,54] X. Shi,[1,49] X. D. Shi,[63,49] J. J. Song,[41] Q. Q. Song,[63,49] W. M. Song,[27,1] Y. X. Song,[38,h] S. Sosio,[66a,66c] S. Spataro,[66a,66c] K. X. Su,[68] P. P. Su,[46] F. F. Sui,[41] G. X. Sun,[1] H. K. Sun,[1] J. F. Sun,[16] L. Sun,[68] S. S. Sun,[1,54] T. Sun,[1,54] W. Y. Sun,[27] W. Y. Sun,[34] X. Sun,[20,i] Y. J. Sun,[63,49] Y. K. Sun,[63,49] Y. Z. Sun,[1] Z. T. Sun,[1] Y. H. Tan,[68] Y. X. Tan,[63,49] C. J. Tang,[45] G. Y. Tang,[1] J. Tang,[50] J. X. Teng,[63,49] V. Thoren,[67] W. H. Tian,[43] Y. T. Tian,[25] I. Uman,[53b] B. Wang,[1] C. W. Wang,[35] D. Y. Wang,[38,h] H. J. Wang,[31,k,l] H. P. Wang,[1,54] K. Wang,[1,49] L. L. Wang,[1] M. Wang,[41] M. Z. Wang,[38,h] Meng Wang,[1,54] W. Wang,[50] W. H. Wang,[68] W. P. Wang,[63,49] X. Wang,[38,h] X. F. Wang,[31,k,l] X. L. Wang,[9,f] Y. Wang,[50] Y. Wang,[63,49] Y. D. Wang,[37] Y. F. Wang,[1,49,54] Y. Q. Wang,[1] Y. Y. Wang,[31,k,l] Z. Wang,[1,49] Z. H. Wang,[63,49] Z. Y. Wang,[1] Ziyi Wang,[54] Zongyuan Wang,[1,54] D. H. Wei,[12] F. Weidner,[60] S. P. Wen,[1] D. J. White,[58] U. Wiedner,[4] G. Wilkinson,[61] M. Wolke,[67] L. Wollenberg,[4] J. F. Wu,[1,54] L. H. Wu,[1] L. J. Wu,[1,54] X. Wu,[9,f] Z. Wu,[1,49] L. Xia,[63,49] H. Xiao,[9,f] S. Y. Xiao,[1] Z. J. Xiao,[34] X. H. Xie,[38,h] Y. G. Xie,[1,49] Y. H. Xie,[6] T. Y. Xing,[1,54] G. F. Xu,[1] Q. J. Xu,[14] W. Xu,[1,54] X. P. Xu,[46] Y. C. Xu,[54] F. Yan,[9,f] L. Yan,[9,f] W. B. Yan,[63,49] W. C. Yan,[71] Xu Yan,[46] H. J. Yang,[42,e] H. X. Yang,[1] L. Yang,[43] S. L. Yang,[54] Y. X. Yang,[12] Yifan Yang,[1,54] Zhi Yang,[25] M. Ye,[1,49] M. H. Ye,[7] J. H. Yin,[1] Z. Y. You,[50] B. X. Yu,[1,49,54] C. X. Yu,[36] G. Yu,[1,54] J. S. Yu,[20,i]

T. Yu,[64] C. Z. Yuan,[1,54] L. Yuan,[2] X. Q. Yuan,[38,h] Y. Yuan,[1] Z. Y. Yuan,[50] C. X. Yue,[32] A. A. Zafar,[65] X. Zeng Zeng,[6] Y. Zeng,[20,i] Z. Zeng,[63,49,n] A. Q. Zhang,[1] B. X. Zhang,[1] Guangyi Zhang,[16] H. Zhang,[63] H. H. Zhang,[50] H. H. Zhang,[27] H. Y. Zhang,[1,49] J. J. Zhang,[43] J. L. Zhang,[69] J. Q. Zhang,[34] J. W. Zhang,[1,49,54] J. Y. Zhang,[1] J. Z. Zhang,[1,54] Jianyu Zhang,[1,54] Jiawei Zhang,[1,54] L. M. Zhang,[52] L. Q. Zhang,[50] Lei Zhang,[35] S. Zhang,[50] S. F. Zhang,[35] Shulei Zhang,[20,i] X. D. Zhang,[37] X. Y. Zhang,[41] Y. Zhang,[61] Y. T. Zhang,[71] Y. H. Zhang,[1,49] Yan Zhang,[63,49] Yao Zhang,[1] Z. H. Zhang,[6] Z. Y. Zhang,[68] G. Zhao,[1] J. Zhao,[32] J. Y. Zhao,[1,54] J. Z. Zhao,[1,49] Lei Zhao,[63,49] Ling Zhao,[1] M. G. Zhao,[36] Q. Zhao,[1] S. J. Zhao,[71] Y. B. Zhao,[1,49] Y. X. Zhao,[25] Z. G. Zhao,[63,49] A. Zhemchugov,[29,a] B. Zheng,[64] J. P. Zheng,[1,49] Y. Zheng,[38,h] Y. H. Zheng,[54] B. Zhong,[34] C. Zhong,[64] L. P. Zhou,[1,54] Q. Zhou,[1,54] X. Zhou,[68] X. K. Zhou,[54] X. R. Zhou,[63,49] X. Y. Zhou,[32] A. N. Zhu,[1,54] J. Zhu,[36] K. Zhu,[1] K. J. Zhu,[1,49,54] S. H. Zhu,[62] T. J. Zhu,[69] W. J. Zhu,[36] W. J. Zhu,[9,f] Y. C. Zhu,[63,49] Z. A. Zhu,[1,54] B. S. Zou,[1] and J. H. Zou[1]

(BESIII Collaboration)

[1]*Institute of High Energy Physics, Beijing 100049, People's Republic of China*
[2]*Beihang University, Beijing 100191, People's Republic of China*
[3]*Beijing Institute of Petrochemical Technology, Beijing 102617, People's Republic of China*
[4]*Bochum Ruhr-University, D-44780 Bochum, Germany*
[5]*Carnegie Mellon University, Pittsburgh, Pennsylvania 15213, USA*
[6]*Central China Normal University, Wuhan 430079, People's Republic of China*
[7]*China Center of Advanced Science and Technology, Beijing 100190, People's Republic of China*
[8]*COMSATS University Islamabad, Lahore Campus, Defence Road, Off Raiwind Road, 54000 Lahore, Pakistan*
[9]*Fudan University, Shanghai 200443, People's Republic of China*
[10]*G.I. Budker Institute of Nuclear Physics SB RAS (BINP), Novosibirsk 630090, Russia*
[11]*GSI Helmholtzcentre for Heavy Ion Research GmbH, D-64291 Darmstadt, Germany*
[12]*Guangxi Normal University, Guilin 541004, People's Republic of China*
[13]*Guangxi University, Nanning 530004, People's Republic of China*
[14]*Hangzhou Normal University, Hangzhou 310036, People's Republic of China*
[15]*Helmholtz Institute Mainz, Staudinger Weg 18, D-55099 Mainz, Germany*
[16]*Henan Normal University, Xinxiang 453007, People's Republic of China*
[17]*Henan University of Science and Technology, Luoyang 471003, People's Republic of China*
[18]*Huangshan College, Huangshan 245000, People's Republic of China*
[19]*Hunan Normal University, Changsha 410081, People's Republic of China*
[20]*Hunan University, Changsha 410082, People's Republic of China*
[21]*Indian Institute of Technology Madras, Chennai 600036, India*
[22]*Indiana University, Bloomington, Indiana 47405, USA*
[23a]*INFN Laboratori Nazionali di Frascati, I-00044 Frascati, Italy*
[23b]*INFN Sezione di Perugia, I-06100 Perugia, Italy*
[23c]*University of Perugia, I-06100 Perugia, Italy*
[24a]*INFN Sezione di Ferrara, I-44122 Ferrara, Italy*
[24b]*University of Ferrara, I-44122 Ferrara, Italy*
[25]*Institute of Modern Physics, Lanzhou 730000, People's Republic of China*
[26]*Institute of Physics and Technology, Peace Avenue 54B, Ulaanbaatar 13330, Mongolia*
[27]*Jilin University, Changchun 130012, People's Republic of China*
[28]*Johannes Gutenberg University of Mainz, Johann-Joachim-Becher-Weg 45, D-55099 Mainz, Germany*
[29]*Joint Institute for Nuclear Research, 141980 Dubna, Moscow region, Russia*
[30]*Justus-Liebig-Universitaet Giessen, II. Physikalisches Institut, Heinrich-Buff-Ring 16, D-35392 Giessen, Germany*
[31]*Lanzhou University, Lanzhou 730000, People's Republic of China*
[32]*Liaoning Normal University, Dalian 116029, People's Republic of China*
[33]*Liaoning University, Shenyang 110036, People's Republic of China*
[34]*Nanjing Normal University, Nanjing 210023, People's Republic of China*
[35]*Nanjing University, Nanjing 210093, People's Republic of China*
[36]*Nankai University, Tianjin 300071, People's Republic of China*
[37]*North China Electric Power University, Beijing 102206, People's Republic of China*
[38]*Peking University, Beijing 100871, People's Republic of China*
[39]*Qufu Normal University, Qufu 273165, People's Republic of China*
[40]*Shandong Normal University, Jinan 250014, People's Republic of China*
[41]*Shandong University, Jinan 250100, People's Republic of China*

[42]Shanghai Jiao Tong University, Shanghai 200240, People's Republic of China
[43]Shanxi Normal University, Linfen 041004, People's Republic of China
[44]Shanxi University, Taiyuan 030006, People's Republic of China
[45]Sichuan University, Chengdu 610064, People's Republic of China
[46]Soochow University, Suzhou 215006, People's Republic of China
[47]South China Normal University, Guangzhou 510006, People's Republic of China
[48]Southeast University, Nanjing 211100, People's Republic of China
[49]State Key Laboratory of Particle Detection and Electronics, Beijing 100049, Hefei 230026, People's Republic of China
[50]Sun Yat-Sen University, Guangzhou 510275, People's Republic of China
[51]Suranaree University of Technology, University Avenue 111, Nakhon Ratchasima 30000, Thailand
[52]Tsinghua University, Beijing 100084, People's Republic of China
[53a]Turkish Accelerator Center Particle Factory Group, Istanbul Bilgi University, HEP Research Center, 34060 Eyup, Istanbul, Turkey
[53b]Near East University, Nicosia, North Cyprus, Mersin 10, Turkey
[54]University of Chinese Academy of Sciences, Beijing 100049, People's Republic of China
[55]University of Groningen, NL-9747 AA Groningen, Netherlands
[56]University of Hawaii, Honolulu, Hawaii 96822, USA
[57]University of Jinan, Jinan 250022, People's Republic of China
[58]University of Manchester, Oxford Road, Manchester M13 9PL, United Kingdom
[59]University of Minnesota, Minneapolis, Minnesota 55455, USA
[60]University of Muenster, Wilhelm-Klemm-Straße 9, 48149 Muenster, Germany
[61]University of Oxford, Keble Road, Oxford OX1 3RH, United Kingdom
[62]University of Science and Technology Liaoning, Anshan 114051, People's Republic of China
[63]University of Science and Technology of China, Hefei 230026, People's Republic of China
[64]University of South China, Hengyang 421001, People's Republic of China
[65]University of the Punjab, Lahore-54590, Pakistan
[66a]University of Turin, I-10125 Turin, Italy
[66b]University of Eastern Piedmont, I-15121 Alessandria, Italy
[66c]INFN, I-10125 Turin, Italy
[67]Uppsala University, Box 516, SE-75120 Uppsala, Sweden
[68]Wuhan University, Wuhan 430072, People's Republic of China
[69]Xinyang Normal University, Xinyang 464000, People's Republic of China
[70]Zhejiang University, Hangzhou 310027, People's Republic of China
[71]Zhengzhou University, Zhengzhou 450001, People's Republic of China

(Received 26 April 2021; accepted 7 July 2021; published 20 August 2021)

The process $e^+e^- \to \phi\eta$ is studied at 22 center-of-mass energy points ($\sqrt{s}$) between 2.00 and 3.08 GeV using 715 pb^{-1} of data collected with the BESIII detector. The measured Born cross section of $e^+e^- \to \phi\eta$

[a]Also at the Moscow Institute of Physics and Technology, Moscow 141700, Russia.
[b]Also at the Novosibirsk State University, Novosibirsk 630090, Russia.
[c]Also at the NRC "Kurchatov Institute," PNPI, 188300 Gatchina, Russia.
[d]Also at Goethe University Frankfurt, 60323 Frankfurt am Main, Germany.
[e]Also at Key Laboratory for Particle Physics, Astrophysics and Cosmology, Ministry of Education; Shanghai Key Laboratory for Particle Physics and Cosmology; Institute of Nuclear and Particle Physics, Shanghai 200240, People's Republic of China.
[f]Also at Key Laboratory of Nuclear Physics and Ion-beam Application (MOE) and Institute of Modern Physics, Fudan University, Shanghai 200443, People's Republic of China.
[g]Also at Harvard University, Department of Physics, Cambridge, Massachusetts 02138, USA.
[h]Also at State Key Laboratory of Nuclear Physics and Technology, Peking University, Beijing 100871, People's Republic of China.
[i]Also at School of Physics and Electronics, Hunan University, Changsha 410082, China.
[j]Also at Guangdong Provincial Key Laboratory of Nuclear Science, Institute of Quantum Matter, South China Normal University, Guangzhou 510006, China.
[k]Also at Frontiers Science Center for Rare Isotopes, Lanzhou University, Lanzhou 730000, People's Republic of China.
[l]Also at Lanzhou Center for Theoretical Physics, Lanzhou University, Lanzhou 730000, People's Republic of China.
[m]Currently at Istinye University, 34010 Istanbul, Turkey.
[n]Also at Wugang No. 3 High School, Wuhan 430080, China.

is found to be consistent with *BABAR* measurements, but with improved precision. A resonant structure around 2.175 GeV is observed with a significance of 6.9σ with mass $(2163.5 \pm 6.2 \pm 3.0)$ MeV/c^2 and width $(31.1^{+21.1}_{-11.6} \pm 1.1)$ MeV, where the first uncertainties are statistical and the second are systematic.

DOI: 10.1103/PhysRevD.104.032007

I. INTRODUCTION

The first observation of the $\phi(2170)$ meson was reported by the *BABAR* Collaboration in the initial-state radiation (ISR) process $e^+e^- \to \gamma_{ISR}\phi\pi^+\pi^-$ [1]. The *BABAR* [2–4], BES [5], Belle [6], and BESIII [7–12] Collaborations also studied $\phi(2170)$ decays. Since the $\phi(2170)$ is produced in e^+e^- collisions, its quantum numbers are $J^{PC} = 1^{--}$. The discovery of the $\phi(2170)$ has sparked extensive discussions about its internal structure. Proposed explanations include an $s\bar{s}g$ hybrid state [13–17], either the 2^3D_1 [18–21] or 3^3S_1 [22,23] $s\bar{s}$ state, an $s\bar{s}s\bar{s}$ tetraquark state [24–32], a $\Lambda\bar{\Lambda}$ molecular state [33–38], a $\phi f_0(980)$ resonance [30,39–41] including final-state interaction effects [7,42], an S-wave threshold effect [42], and a $X(2240)$ state [43]. None of these explanations has been able to describe all experimental observations. Therefore, the nature of the $\phi(2170)$ still needs to be clarified by further theoretical and experimental efforts.

For different hypotheses regarding the internal structure of the $\phi(2170)$, certain decay modes such as $\phi(2170) \to \phi\eta$ [3,15,18,19] can have decay rates that vary strongly across those models. According to the Okubo-Zweig-Iizuka (OZI) rule [44], excited ϕ mesons are predicted to decay with a considerable fraction into the $s\bar{s}$ modes $\phi\eta$ and $\phi\eta'$ [22,23]. Both the 2^3D_1 [18,19] and 3^3S_1 [22,23] $s\bar{s}$ states as well as $s\bar{s}s\bar{s}$ [24–32] tetraquark states favor the $\phi\eta$ and $\phi\eta'$ decay modes according to model calculations. Consequently, $e^+e^- \to \phi\eta$ is an excellent channel to study excited ϕ states [44].

The *BABAR* Collaboration observed evidence of the $\phi(2170)$ in the measurement of the cross section of $e^+e^- \to \gamma_{ISR}\phi\eta$ using the ISR method [3], and also found a hint of the $\phi(2170)$ in the process $e^+e^- \to \gamma_{ISR}\phi\eta'$ [45]. Assuming that the observed structure in the process $e^+e^- \to \phi\eta$ is the $\phi(2170)$, *BABAR* measured a partial width of $\mathcal{B}^{\phi(2170)}_{\phi\eta}\Gamma^{\phi(2170)}_{e^+e^-} = (1.7 \pm 0.7 \pm 1.3)$ eV [3]. In recent studies of the processes $e^+e^- \to K^+K^-$ [8,46], ϕK^+K^- [9], $K^+K^-\pi^0\pi^0$ [10], $\omega\eta$ [12], and $\phi\eta'$ [11] by the BESIII Collaboration, a clear structure around 2.2 GeV is observed in the line shape of the measured cross sections.

The ratio between the $\phi\eta$ and $\phi\eta'$ partial widths is an important observable to assess the $\phi(2170)$ as a hybrid state. An $s\bar{s}g$ hybrid state is expected to have a stronger coupling to $\phi\eta$, with the partial width expected to be larger than that to $\phi\eta'$ by factors ranging from 3 up to 200 [14,15]. The resulting partial width in the study of $e^+e^- \to \phi\eta'$ at BESIII is found to be $\mathcal{B}^{\phi(2170)}_{\phi\eta'}\Gamma^{\phi(2170)}_{e^+e^-} = (7.1 \pm 0.7 \pm 0.7)$ eV [11]. The precision of the ratio of partial widths between the decays to $\phi\eta$ and $\phi\eta'$ of $\mathcal{B}^{\phi(2170)}\Gamma^{\phi(2170)}_{e^+e^-}$ provides a strong benchmark for theoretical models aiming to explain the nature of the $\phi(2170)$. Hence, a new measurement of the cross section of the process $e^+e^- \to \phi\eta$ is important in order to improve our understanding of the nature of the $\phi(2170)$ resonance.

In this paper, we present an improved measurement of the Born cross section ($\sigma^{\rm Born}_{\phi\eta}$) of the process $e^+e^- \to \phi\eta$ at 22 ($\sqrt{s}$) in the range between 2.00 and 3.08 GeV with a data sample corresponding to an integrated luminosity of 715 pb^{-1} collected with the BESIII experiment.

II. BESIII EXPERIMENT AND MONTE CARLO SIMULATION

The BESIII detector is a magnetic spectrometer [47] located at the Beijing Electron Positron Collider (BEPCII) [48]. The cylindrical core of the BESIII detector consists of a helium-based multilayer drift chamber (MDC), a plastic scintillator time-of-flight system (TOF), and a CsI(Tl) electromagnetic calorimeter (EMC), which are all enclosed in a superconducting solenoidal magnet providing a 1.0 T magnetic field. The solenoid is supported by an octagonal flux-return yoke instrumented with resistive plate counters interleaved with steel, which serve as muon identifiers. The acceptance of charged particles and photons is 93% of the full solid angle. The charged-particle momentum resolution at 1 GeV/c is 0.5%, and the dE/dx resolution is 6% for electrons from Bhabha scattering. The EMC measures photon energies with a resolution of 2.5% (5%) at 1 GeV in the barrel (end cap) region. The time resolution of the TOF barrel part is 68 ps, while that of the end cap part is 110 ps.

The detector response, including the interaction of secondary particles with the detector material, is simulated using GEANT4-based [49] Monte Carlo (MC) software. MC simulation samples of 2.5×10^6 $e^+e^- \to \phi\eta$ events per energy point generated by using P-waves in the production process with the CONEXC [50] generator are used for the efficiency determination and to calculate the correction factors for radiative effects up to next-to-leading order (NLO), as well for the effect of vacuum polarization (VP). MC samples of inclusive hadronic events generated with CONEXC combined with LUARLW [50] are used for background studies.

III. EVENT SELECTION AND BACKGROUND ANALYSIS

To select $e^+e^- \to \phi\eta$, the ϕ and η candidates are reconstructed through their decays to K^+K^- and $\gamma\gamma$, respectively. Selected events must have exactly two charged tracks with opposite charge. Tracks are reconstructed using the MDC, and all track candidates have to be within the MDC acceptance of $|\cos\theta| < 0.93$, where θ is the polar angle with respect to the symmetry axis of the drift chamber. Additionally, both tracks are required to have their point of closest approach to the interaction point be within 10 cm along the beam direction and 1 cm in the transverse plane. The TOF and the dE/dx information are combined to calculate a particle identification (PID) likelihood for the π, K, and p hypotheses. For both tracks, it is required that the likelihood of a kaon assignment be larger than the two alternative hypotheses.

Photon candidates are selected from showers in the EMC that are not associated with charged tracks. Good photon candidates reconstructed in the barrel part of the EMC must have a polar angle within $|\cos\theta| < 0.8$, while photon candidates reconstructed in the end caps must have a polar angle within $0.86 < |\cos\theta| < 0.92$. In order to suppress the background from ISR processes, the energy of all photon candidates is required to be larger than 70 MeV. To suppress electronic noise and energy deposits unrelated to the event, the timing information from the EMC is required to be within 700 ns of the event start time for all photon candidates.

A four-constraint (4C) kinematic fit is applied using the hypothesis $e^+e^- \to K^+K^-\gamma\gamma$, constraining the measured four-momenta of all particles to the initial center-of-mass (c.m.) four-momentum. For events with more than two good photon candidates, the combination with the smallest χ^2 of the kinematic fit is retained for further study. Only events with $\chi^2_{4C}(K^+K^-\gamma\gamma) < 100$ are kept. In order to suppress background contributions from the reaction $e^+e^- \to \gamma_{ISR}\phi$, $\phi \to K^+K^-$, where γ_{ISR} is the detected ISR photon, a second kinematic fit is used testing the $e^+e^- \to K^+K^-\gamma$ hypothesis. Events are rejected if the χ^2 of the kinematic fit to the $e^+e^- \to K^+K^-\gamma$ hypothesis is smaller than the one for the signal hypothesis. The distribution of the invariant mass of the two kaons $[M(K^+K^-)]$ versus the invariant mass of the two photons $[M(\gamma\gamma)]$ is shown in Fig. 1 for the data at a $(\sqrt{s})$ of 2.125 GeV using the above selection criteria. An enhancement at the η and ϕ meson masses is observed. Candidate events of $e^+e^- \to \phi\eta$ are required to be within the combined η and ϕ signal region, defined as $|M(\gamma\gamma) - m_\eta| < 30\,\mathrm{MeV}/c^2$, $0.98 < M(K^+K^-) < 1.08\,\mathrm{GeV}/c^2$, where m_η is the mass of η meson as listed by the PDG [51], and 30 MeV/c^2 corresponds to 3 times the detector resolution at the η mass.

The main sources of the remaining background are processes of the type $e^+e^- \to K^+K^-\eta$ (where the K^+K^- pair does not originate from a ϕ decay), $e^+e^- \to K^+K^-\pi^0$, and $e^+e^- \to K^+K^-\pi^0\pi^0$. Possible contaminations are estimated to be less than 1.0% from studies performed on inclusive hadronic MC samples. After selecting η candidates using the invariant mass $M(\gamma\gamma)$, background contributions are highly suppressed and do not exhibit narrow structures in $M(K^+K^-)$ so that they can be described by a smooth polynomial function.

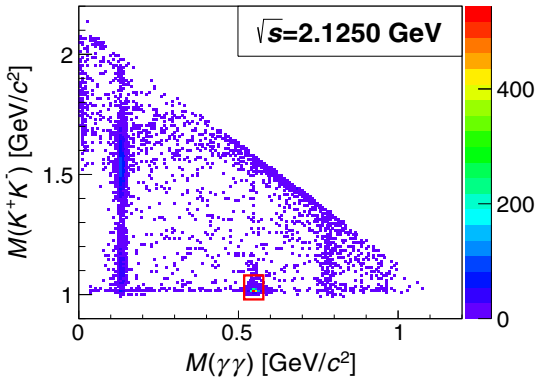

FIG. 1. Distribution of $m(K^+K^-)$ versus $m(\gamma\gamma)$ at $\sqrt{s} = 2.125$ GeV. The red rectangle indicates the signal region.

IV. CROSS SECTIONS OF $e^+e^- \to \phi\eta$

A. Signal yields

The number of events of the process $e^+e^- \to \phi\eta$ is determined by an unbinned maximum-likelihood fit to the K^+K^- invariant mass with a signal shape, which is parametrized by a P-wave relativistic Breit-Wigner function convolved with a Gaussian function. The background shape is described by a first-order polynomial. According to Ref. [52], the P-wave relativistic Breit-Wigner amplitude for $\phi \to K^+K^-$ is

$$A[M(K^+K^-)] = p_K\{M(K^+K^-)^2 - m_\phi^2 + iM(K^+K^-) \cdot \Gamma[M(K^+K^-)]\}^{-1} \cdot \frac{B(p_K)}{B(p'_K)}, \quad (1)$$

where m_ϕ is fixed to the mass of the ϕ meson [51], p_K is the kaon momentum in the ϕ rest frame, and p'_K is the kaon momentum at the nominal ϕ mass. The width $\Gamma[M(K^+K^-)]$ is given by

$$\Gamma[M(K^+K^-)] = \left(\frac{p_K}{p'_K}\right)^3 \left[\frac{M(K^+K^-)}{m_\phi}\right] \Gamma_0 \left[\frac{B(p_K)}{B(p'_K)}\right], \quad (2)$$

where Γ_0 is fixed to the nominal width of the ϕ meson [51] and $B(p)$ is the P-wave Blatt-Weisskopf form factor with $B(p) = \sqrt{\frac{2(Rp)^2}{1+(Rp)^2}}$, where $R = 3\ \mathrm{GeV}^{-1}\,c$ is chosen as the radius in the calculation of the centrifugal barrier factor. The amplitude squared convolved with the Gaussian function is added incoherently to the background polynomial. The parameters of the polynomial and the Gaussian

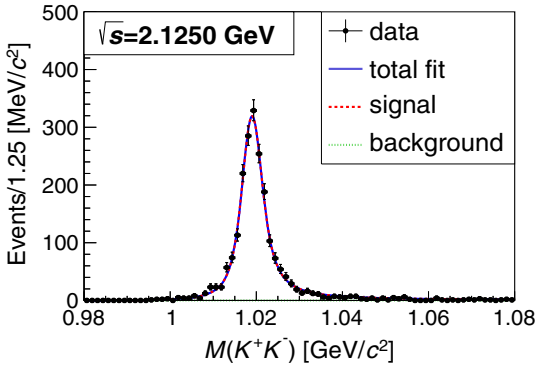

FIG. 2. The invariant mass of the K^+K^- pair after selection of the η meson candidate for the $\sqrt{s}$ of 2.125 GeV. Black dots represent experimental data, and the blue solid curve is the total fit result, while the red dashed and green dotted curves show the individual signal and background components, respectively.

function are free in the fit. The latter is used to compensate for absolute resolution and an offset of the mass scaling in data. The fit result for the data at $\sqrt{s} = 2.125$ GeV is shown in Fig. 2, while the signal event yields $N_{\rm Signal}$ for all energy points are summarized in Table I.

B. Efficiency and radiative corrections

With $N_{\rm Signal}$ determined, the Born cross section $\sigma^{\rm Born}_{\phi\eta}(s)$ of the process $e^+e^- \to \phi\eta$ at the c.m. energy squared s can be determined using

$$\sigma^{\rm Born}_{\phi\eta}(s) = \frac{N_{\rm Signal}}{\mathcal{L}\cdot\epsilon\cdot(1+\delta)\cdot\frac{1}{(1-\Pi)^2}\cdot\mathcal{B}}, \quad (3)$$

where $\mathcal{L}$ is the integrated luminosity measured with large-angle Bhabha scattering [53], ϵ is the reconstruction efficiency, $(1+\delta)$ is the radiative correction factor, and $\frac{1}{(1-\Pi)^2}$ is the VP correction factor. The explicit $(\sqrt{s})$ dependence of those variables is omitted here. The total branching fraction $\mathcal{B}$ is the product of the branching fractions for the decays contained in the full decay chain $\mathcal{B} = \mathcal{B}(\phi \to K^+K^+)\cdot\mathcal{B}(\eta \to \gamma\gamma) = (19.39 \pm 0.22)\%$ [51]. The product $\epsilon(1+\delta)$ is determined in an iterative procedure. At each step of the iteration, a set of 1000 MC samples is produced, taking into account the fit to the Born cross section introduced in Sec. V. The MC samples are produced by sampling the model parameters according to a Gaussian distribution using the uncertainties of the model parameters as obtained in the fit as the width of the Gaussian distribution. Each of the 1000 MC samples gives a new value of $\epsilon(1+\delta)$. The mean of those 1000 values is used to recalculate the Born cross section. This process is repeated until the resulting Born cross section converges. After two iterations, the observed change in the Born cross section $\sigma^{\rm Born}_{\phi\eta}(s)$ is smaller than the uncertainty of the generator, which is 0.5%. The efficiency, the radiative and VP correction factors, and the results for $\sigma^{\rm Born}_{\phi\eta}$ are summarized in Table I.

TABLE I. The integrated luminosity $\mathcal{L}$, the number of $\phi\eta$ events $N_{\rm Signal}$, efficiency ϵ, radiative correction factor $(1+\delta)$, VP correction factor $\frac{1}{(1-\Pi)^2}$, and the Born cross section $\sigma^{\rm Born}_{\phi\eta}$ for the different $\sqrt{s}$. The statistical uncertainty on the efficiency is negligible.

$\sqrt{s}$[GeV]	$\mathcal{L}$[pb^{-1}]	$N_{\rm Signal}$	ϵ[%]	$(1+\delta)$	$\frac{1}{(1-\Pi)^2}$	$\sigma^{\rm Born}_{\phi\eta}$[pb]
2.0000	10.1 ± 0.1	237.0 ± 15.4	21.5	1.113	1.037	$489.9 \pm 31.8 \pm 20.0$
2.0500	3.34 ± 0.03	72.1 ± 8.5	22.4	1.131	1.038	$422.4 \pm 49.8 \pm 19.0$
2.1000	12.2 ± 0.1	252.0 ± 15.9	23.3	1.135	1.039	$389.2 \pm 24.5 \pm 16.6$
2.1250	108 ± 1	2097.0 ± 45.8	23.9	1.120	1.039	$358.6 \pm 7.8 \pm 14.0$
2.1500	2.84 ± 0.02	60.8 ± 7.8	24.7	1.090	1.040	$394.1 \pm 50.5 \pm 16.7$
2.1750	10.6 ± 0.1	146.7 ± 12.6	24.4	1.348	1.040	$208.4 \pm 17.9 \pm 11.0$
2.2000	13.7 ± 0.1	161.0 ± 12.7	21.6	1.358	1.040	$198.9 \pm 15.7 \pm 8.2$
2.2324	14.5 ± 0.1	125.9 ± 11.9	22.4	1.315	1.041	$145.9 \pm 13.8 \pm 7.3$
2.3094	21.1 ± 0.1	201.1 ± 14.2	23.0	1.314	1.041	$156.0 \pm 11.0 \pm 6.6$
2.3864	22.5 ± 0.2	197.5 ± 15.1	23.3	1.342	1.041	$138.8 \pm 10.6 \pm 5.9$
2.3960	66.9 ± 0.5	502.8 ± 23.4	23.4	1.346	1.041	$118.1 \pm 5.5 \pm 5.1$
2.4000	3.42 ± 0.03	26.3 ± 5.3	23.9	1.348	1.041	$118.6 \pm 24.0 \pm 6.1$
2.6444	33.7 ± 0.2	156.0 ± 12.5	23.1	1.475	1.039	$67.3 \pm 5.4 \pm 2.6$
2.6464	34.0 ± 0.3	157.0 ± 12.5	23.0	1.476	1.039	$67.5 \pm 5.4 \pm 2.8$
2.9000	105 ± 1	262.8 ± 16.2	21.9	1.639	1.033	$34.8 \pm 2.1 \pm 1.7$
2.9500	15.9 ± 0.1	29.0 ± 5.4	21.4	1.677	1.029	$25.5 \pm 4.7 \pm 1.1$
2.9810	16.1 ± 0.1	29.9 ± 5.7	21.3	1.703	1.025	$25.8 \pm 4.9 \pm 1.4$
3.0000	15.9 ± 0.1	29.1 ± 5.6	21.1	1.720	1.021	$25.6 \pm 4.9 \pm 1.8$
3.0200	17.3 ± 0.1	25.0 ± 5.0	20.9	1.741	1.014	$20.2 \pm 4.0 \pm 1.7$
3.0500	14.9 ± 0.1	21.0 ± 4.6	20.8	1.782	0.996	$19.7 \pm 4.3 \pm 0.8$
3.0600	15.0 ± 0.1	29.1 ± 5.4	20.6	1.803	0.984	$27.4 \pm 5.1 \pm 1.3$
3.0800	157 ± 1	298.5 ± 17.6	19.4	1.901	0.915	$29.1 \pm 1.7 \pm 1.2$

TABLE II. Relative systematic uncertainties (in %) of the measurement of $\sigma^{\rm Born}_{\phi\eta}$ from the tracking efficiency (Trk), PID efficiency (PID), photon detection (γ detect), luminosity (Lum), the kinematic fit (KinFit), η selection (η range), fit range (Fit range), signal shape (Signal), background shape (Background), ϕ peaking background (Side), radiative correction [$\epsilon(1+\delta)$], and branching fractions ($\mathcal{B}$). The total uncertainty is obtained by summing the individual contributions in quadrature.

$\sqrt{s}$ [GeV]	Trk	PID	γ detect	Lum	KinFit	η range	Fit range	Signal	Background	Side	$\epsilon(1+\delta)$	$\mathcal{B}$	Total
2.0000	2.0	2.0	2.0	0.7	0.0	1.0	0.0	0.5	1.1	0.5	0.5	1.1	4.1
2.0500	2.0	2.0	2.0	0.8	1.4	1.3	1.5	0.0	0.1	0.0	0.5	1.1	4.5
2.1000	2.0	2.0	2.0	0.7	1.2	0.6	0.1	0.5	1.0	1.1	0.5	1.1	4.3
2.1250	2.0	2.0	2.0	0.9	0.8	0.3	0.0	0.2	0.1	0.4	0.5	1.1	3.9
2.1500	2.0	2.0	2.0	0.9	0.2	1.5	0.2	0.9	0.6	0.0	0.5	1.1	4.2
2.1750	2.0	2.0	2.0	0.9	0.4	2.8	0.1	0.8	1.0	1.2	1.6	1.1	5.3
2.2000	2.0	2.0	2.0	0.7	0.5	0.8	0.3	0.6	1.3	0.0	0.5	1.1	4.1
2.2324	2.0	2.0	2.0	0.6	0.6	1.1	2.3	1.3	1.1	1.3	0.5	1.1	5.0
2.3094	2.0	2.0	2.0	0.7	0.1	1.2	0.0	0.0	0.1	1.5	0.5	1.1	4.2
2.3864	2.0	2.0	2.0	0.8	0.7	0.7	1.3	1.0	0.2	0.5	0.5	1.1	4.3
2.3960	2.0	2.0	2.0	0.7	0.8	1.1	0.4	0.7	1.3	0.8	0.5	1.1	4.4
2.4000	2.0	2.0	2.0	0.7	0.2	1.8	2.7	0.7	0.9	0.0	0.5	1.1	5.1
2.6444	2.0	2.0	2.0	0.6	0.1	0.6	0.5	0.4	0.8	0.3	0.5	1.1	3.9
2.6464	2.0	2.0	2.0	0.8	0.0	1.3	0.1	0.7	0.5	1.1	0.5	1.1	4.2
2.9000	2.0	2.0	2.0	0.9	0.4	0.9	0.2	0.0	0.9	2.7	0.5	1.1	4.9
2.9500	2.0	2.0	2.0	0.9	0.4	1.8	0.3	0.8	0.4	0.0	0.5	1.1	4.3
2.9810	2.0	2.0	2.0	0.6	0.7	1.8	3.5	0.9	0.6	0.0	0.5	1.1	5.6
3.0000	2.0	2.0	2.0	0.7	1.1	1.8	1.8	0.7	0.6	5.2	0.5	1.1	7.0
3.0200	2.0	2.0	2.0	0.7	4.0	6.3	0.5	0.0	0.0	0.0	0.5	1.1	8.3
3.0500	2.0	2.0	2.0	0.7	0.0	1.7	0.9	0.0	0.1	0.0	0.5	1.1	4.2
3.0600	2.0	2.0	2.0	0.9	0.7	2.3	0.0	1.3	1.1	0.0	0.5	1.1	4.8
3.0800	2.0	2.0	2.0	0.6	0.6	0.5	0.6	0.2	0.8	1.4	0.5	1.1	4.2

C. Systematic uncertainties

Several sources of systematic uncertainties are considered in the determination of $\sigma^{\rm Born}_{\phi\eta}$. The uncertainties associated with the knowledge of the tracking efficiency of the two charged tracks as well as those from the PID efficiency are studied with a $e^+e^- \to K^+K^-\pi^+\pi^-$ control sample. The difference of the efficiency measured in data and MC is assigned as the uncertainty, and it is found to be 1.0% per track for both tracking and PID efficiency [8]. The uncertainty due to photon reconstruction efficiency is 1.0% per photon [54]. The uncertainty of the luminosity measurement is smaller than 1.0% [53]. The uncertainty associated with the kinematic fit is estimated by not using the correction of the helix parameters of the charged tracks described in detail in Ref. [55] and taking the difference to the nominal result as the uncertainty. In order to estimate the contribution from the η selection, the mass window is varied from $|M(\gamma\gamma) - m_\eta| < 3\sigma$ to 2.5σ and 3.5σ, and the larger difference to the nomimal result is taken as the uncertainty. The systematic uncertainty of the signal yield is estimated by varying the fit range from $(0.98, 1.08)$ GeV/c^2 to $(0.99, 1.09)$ GeV/c^2, where the difference to the nominal result is the uncertainty. The uncertainty related to the signal shape is estimated with an alternative fit using the ϕ MC shape convolved with a Gaussian function. The uncertainty due to background shape is estimated with an alternative fit using an Argus function [56] instead of a polynomial. The uncertainty due to ϕ peaking background is estimated by investigating the η sideband, which is defined as $40\,\mathrm{MeV}/c^2 < |M(\gamma\gamma) - m_\eta| < 150\,\mathrm{MeV}/c^2$. We take the difference of the normalized number of the events from a signal fit to the sideband region and the number of events estimated from MC as systematic uncertainties. The uncertainty in $\epsilon(1+\delta)$ arises from the accuracy of the radiator function, which is about 0.5% [57], and has an additional contribution from the parametrization of the $\sigma^{\rm Born}_{\phi\eta}(s)$ line shape, which is taken as the standard deviation of the fit to the sampled parameters. The two contributions are summed in quadrature. The uncertainties of the branching fractions of intermediate states are 1.1% [51]. Assuming that these contributions to the systematic uncertainties are uncorrelated, the total systematic uncertainties are obtained by adding the individual uncertainties in quadrature. The resulting values for all $\sqrt{s}$ are shown in Table II. The total systematic uncertainties on $\sigma^{\rm Born}_{\phi\eta}$ range from 3.9% to 8.3%.

V. LINE SHAPE OF $e^+e^- \to \phi\eta$

A. Fit of the line shape

To study a possible resonant behavior in $e^+e^- \to \phi\eta$, a least χ^2 fit taking into account the correlation between systematic uncertainties for different ($\sqrt{s}$) is performed to the measured values of the Born cross section $\sigma^{\rm Born}_{\phi\eta}$.

Previous results from the *BABAR* Collaboration [3] are also included to be able to describe the low-energy behavior of the cross section. Following Ref. [3] and assuming that the reaction proceeds mostly through the decay of the two resonances $\phi(1680)$ and $\phi(2170)$, the line shape is fitted using a coherent sum of two phase-space factor modified Breit-Wigner functions and a nonresonant term:

$$\sigma^{\rm Born}_{\phi\eta}(s) = 12\pi\mathcal{P}_{\phi\eta}(s)|A^{\rm n.r.}_{\phi\eta}(s) + A^{\phi(1680)}_{\phi\eta}(s) + A^{\phi(2170)}_{\phi\eta}(s)|^2, \tag{4}$$

where $\mathcal{P}_{\phi\eta}(s)$ is the phase-space factor of the $\phi\eta$ system, $A^{\rm n.r.}_{\phi\eta}(s)$ describes the nonresonant contribution, and $A^{\phi(1680)}_{\phi\eta}(s)$ and $A^{\phi(2170)}_{\phi\eta}(s)$ are the two vector resonances. For the phase space for the $\phi\eta$ system, we use

$$\mathcal{P}_{\phi\eta}(s) = \left[\frac{(s + m^2_\phi - m^2_\eta)^2 - 4m^2_\phi s}{s}\right]^{\frac{3}{2}}. \tag{5}$$

A reasonable description of the nonresonant contribution is given by the power-law dependence $A^{\rm n.r.}_{\phi\eta}(s) = a_0/s^{a_1}$. We describe the $\phi(1680)$ resonance using Breit-Wigner amplitude

$$A^{\phi(1680)}_{\phi\eta}(s) = \sqrt{\mathcal{B}^{\phi(1680)}_{\phi\eta}\Gamma^{\phi(1680)}_{e^+e^-}} \times \frac{\sqrt{\frac{\Gamma_{\phi(1680)}}{\mathcal{P}_{\phi\eta}(m^2_{\phi(1680)})}}}{m^2_{\phi(1680)} - s - i\sqrt{s}\Gamma_{\phi(1680)}(s)}, \tag{6}$$

with partial width $\mathcal{B}^{\phi(1680)}_{\phi\eta}\Gamma^{\phi(1680)}_{e^+e^-}$, mass $m_{\phi(1680)}$, and width $\Gamma_{\phi(1680)}$. The width $\Gamma_{\phi(1680)}$ on the denominator uses an energy-dependent width [3]:

$$\Gamma_{\phi(1680)}(s) = \Gamma_{\phi(1680)}\left[\frac{\mathcal{P}_{\phi\eta}(s)}{\mathcal{P}_{\phi\eta}(m^2_{\phi(1680)})}\mathcal{B}^{\phi(1680)}_{\phi\eta} + (1 - \mathcal{B}^{\phi(1680)}_{\phi\eta})\right]. \tag{7}$$

In the fit, the previous results from the *BABAR* Collaboration [3] are included to be able to also describe the low-energy behavior (<2 GeV) of the cross section where we have no data. The parameters of the $\phi(1680)$, such as mass ($m_{\phi(1680)} = 1709$ MeV/c^2), width ($\Gamma_{\phi(1680)} = 369$ MeV), and branching fraction ($\Gamma^{\phi(1680)}_{e^+e^-}\mathcal{B}^{\phi(1680)}_{\phi\eta} = 138$ eV), are fixed to the results from Ref. [3]. The $\phi(2170)$ is described using Breit-Wigner amplitude

$$A^{\phi(2170)}_{\phi\eta}(s) = \sqrt{\mathcal{B}^{\phi(2170)}_{\phi\eta}\Gamma^{\phi(2170)}_{e^+e^-}} \times \frac{\sqrt{\frac{\Gamma_{\phi(2170)}}{\mathcal{P}_{\phi\eta}(m^2_{\phi(2170)})}}e^{i\Psi_{\phi(2170)}}}{m^2_{\phi(2170)} - s - i\sqrt{s}\Gamma_{\phi(2170)}} \cdot \frac{B(p)}{B(p')}, \tag{8}$$

with partial width $\mathcal{B}^{\phi(2170)}_{\phi\eta}\Gamma^{\phi(2170)}_{e^+e^-}$, mass $m_{\phi(2170)}$, width $\Gamma_{\phi(2170)}$, and relative phase angle to the nonresonant component $\Psi_{\phi(2170)}$. $B(p)$ is the P-wave Blatt-Weisskopf form factor, p is the breakup momentum corresponding to the $(\sqrt{s})$, and p is the breakup momentum at the $\phi(2170)$ mass.

The fit has two solutions with identical mass and width of the resonance. The fit quality is estimated by χ^2, where the best fit gives a $\chi^2/{\rm n.d.f} = 0.9$, with ${\rm n.d.f} = 97$ being the number of degrees of freedom. The mass and width of $\phi(2170)$ are determined to be $m_{\phi(2170)} = (2163.5 \pm 6.2)$ MeV/c^2 and $\Gamma_{\phi(2170)} = (31.1^{+21.1}_{-11.6})$ MeV from our fit, illustrated in Fig. 3. The significance of the $\phi(2170)$ resonance is determined to be 6.9σ. This is obtained by comparing the change of $\Delta\chi^2 = 59.05$ with [blue solid line in Figs. 3(a)–3(d)] and without [gray dotted line in Figs. 3(a)–3(d)] the resonance in the fit and taking the change of the number of degrees of freedom $\Delta{\rm n.d.f} = 4$ into account. The cross section and the fit results are summarized in Table III and shown in Fig. 3. Figures 3(a) and 3(c) are solution I; Figs. 3(b) and 3(d) are solution II. Figure 3(b) shows the same data subtracting the fit result that is obtained without inclusion of the $\phi(2170)$. It is obvious that an additional resonant structure around 2.175 GeV is needed.

B. Systematic uncertainties

For the systematic uncertainties of the resonance parameters, we examine effects from the choice of the model for the nonresonant contribution and the choice of the fit range. For the model dependence of the nonresonant contribution, $A^{\rm n.r.}_{\phi\eta}(s) = a_0/s$ is used instead, resulting in differences of 3.0 MeV/c^2 and 0.1 MeV for mass and width, respectively. For the dependence on the fit range, we set aside the energy points 2.00 and 3.08 GeV, resulting in differences of 0.3 MeV/c^2 and 1.1 MeV for mass and width, respectively. The total systematic uncertainties are thus 3.0 MeV/c^2 and 1.1 MeV for mass and width, respectively.

VI. SUMMARY AND DISCUSSION

This paper presents the most accurate measurement of the Born cross section of $e^+e^- \to \phi\eta$, at 22 c.m. energies in the interval 2.00 to 3.08 GeV. A resonant structure is observed in the $\sigma^{\rm Born}_{\phi\eta}$ line shape. We determine the parameters of this resonance to be $m_{\phi(2170)} = (2163.5 \pm 6.2 \pm 3.0)$ MeV/c^2 and $\Gamma_{\phi(2170)} = (31.1^{+21.1}_{-11.6} \pm 1.1)$ MeV. Here, the first uncertainties are statistical and the second ones are systematic. The significance is larger than 6.9σ. Compared to a previous measurement by the *BABAR* experiment [3], the mass value reported here is significantly larger. While similar resonances have been observed in many different channels, the observed decay widths vary significantly.

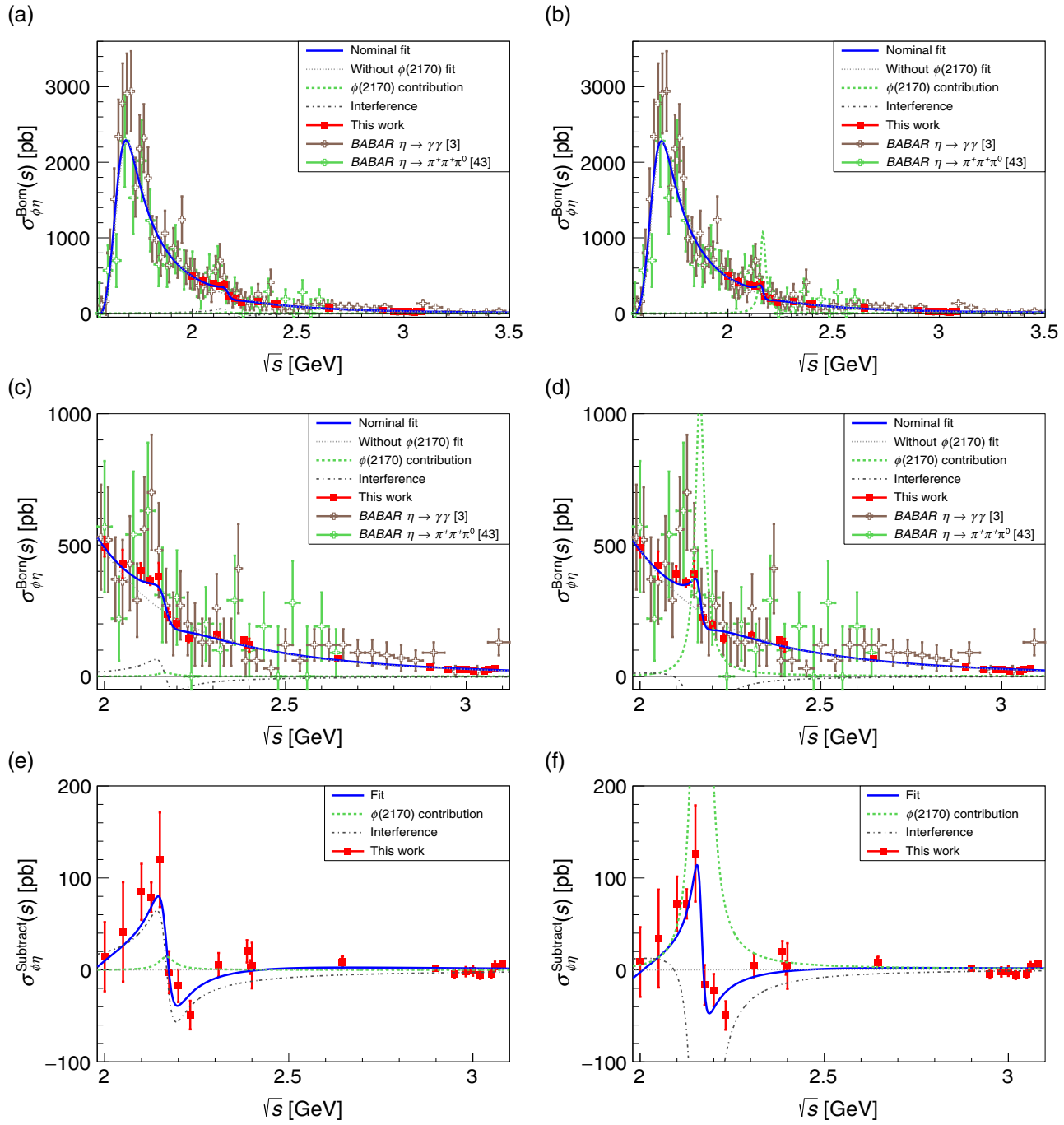

FIG. 3. Results from this work (red solid squares) including statistical and systematic uncertainties for the $e^+e^- \to \phi\eta$ cross section and a fit to the combined data of *BABAR* and this work (blue solid line). Panels (a) and (c) show Solution I; panels (b) and (d) show Solution II. Panels (e) and (f) show the cross section and the nominal fit after subtraction of the fit curve without inclusion of the $\phi(2170)$ for (e) Solution I and (f) Solution II. Also shown are previously published measurements from *BABAR* ($\eta \to \gamma\gamma$) [3] and *BABAR* ($\eta \to \pi^+\pi^-\pi^0$) [45].

The fitted result is compared with the parameters of the $\phi(2170)$ state measured by previous experiments via various processes as shown in Fig. 4. The results obtained in this paper are consistent with the world average parameters of the $\phi(2170)$. However, differences to other individual measurements in different channels can be sizable. Among the existing measurements, the result of this measurement yields the smallest width of the $\phi(2170)$ resonance observed so far.

In principle, the resonance observed in this work could also be an excited ω. However, according to the OZI rule [44], intermediate ω-like resonances should be highly

TABLE III. Parameters for resonances $\phi(2170)$ obtained by fitting.

Parameter	Solution I	Solution II
χ^2/n.d.f.	86.8/97	
a_0	$-0.11^{+0.09}_{-0.22}$	-0.24 ± 0.58
a_1	$1.91^{+0.61}_{-0.76}$	$2.54^{+2.86}_{-1.55}$
$\mathcal{B}^{\phi(2170)}_{\phi\eta}\Gamma^{\phi(2170)}_{e^+e^-}$	$0.24^{+0.12}_{-0.07}$ eV	$10.11^{+3.87}_{-3.13}$ eV
$m_{\phi(2170)}$	2163.5 ± 6.2 MeV/c^2	
$\Gamma_{\phi(2170)}$	$31.1^{+21.1}_{-11.6}$ MeV	
$\Phi_{\phi(2170)}$	$1.82^{+0.35}_{-0.31}$	$-2.92^{+0.05}_{-0.06}$

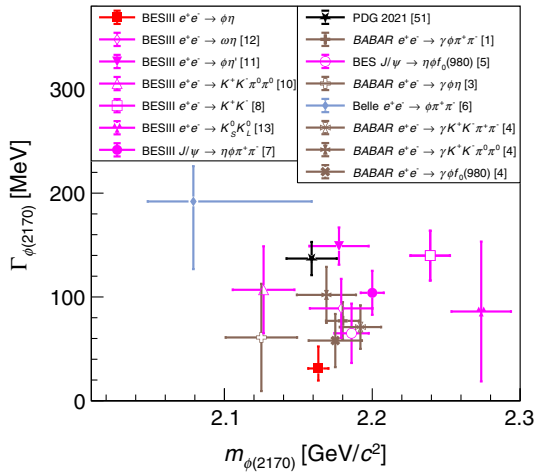

FIG. 4. The parameters of the $\phi(2170)$ state obtained from different processes compared to those obtained in this work in the $e^+e^- \to \phi\eta$ process.

suppressed in the $\phi\eta$ channel. The widths of vector states $\omega(2205)$, $\omega(2290)$, and $\omega(2330)$ listed in PDG [51] are much larger than the results in $\phi\eta$ mode. The mass and width measured in this work do not agree with those of the ρ-like resonance found in $e^+e^- \to \omega\pi^0$ by BESIII [$m_{\phi(2170)} = (2034 \pm 13 \pm 9)$ MeV/c^2, $\Gamma_{\phi(2170)} = (234 \pm 30 \pm 25)$ MeV] [12]. ρ-like contributions should be suppressed due to the isoscalar nature of the $\phi\eta$ channel. Our results agree with those of ρ-like resonance found in a recent work $e^+e^- \to \eta'\pi^+\pi^-$ by BESIII [$m_{\phi(2170)} = (2108 \pm 46 \pm 25)$ MeV/c^2, $\Gamma_{\phi(2170)} = (138 \pm 36 \pm 30)$ MeV] [58] to within 2 standard deviations.

ACKNOWLEDGMENTS

The BESIII collaboration thanks the staff of BEPCII and the IHEP computing center and the supercomputing center of USTC for their strong support. This work is supported in part by the National Key R&D Program of China under Contracts No. 2020YFA0406400 and No. 2020YFA0406300; the National Natural Science Foundation of China (NSFC) under Contracts No. 11625523, No. 11635010, No. 11735014, No. 11822506, No. 11835012, No. 11935015, No. 11935016, No. 11935018, No. 11961141012, No. 12005219, No. 12022510, No. 12025502, No. 12035009, No. 12035013, No. 12061131003, No. 11705192, No. 11875115, No. 11875262, No. 11950410506, and No. 12061131003; the Chinese Academy of Sciences (CAS) Large-Scale Scientific Facility Program; Joint Large-Scale Scientific Facility Funds of the NSFC and CAS under Contracts No. U1732263, No. U1832207, No. U1832103, and No. U2032111; the CAS Key Research Program of Frontier Sciences under Contract No. QYZDJ-SSW-SLH040; the 100 Talents Program of CAS; Institute of Nuclear and Particle Physics and Shanghai Key Laboratory for Particle Physics and Cosmology; ERC under Contract No. 758462; the European Union Horizon 2020 research and innovation programme under Marie Sklodowska-Curie Grant Agreement No. 894790; German Research Foundation DFG under Contract No. 443159800; the Collaborative Research Center CRC 1044, FOR 2359, FOR 2359, GRK 214; Istituto Nazionale di Fisica Nucleare, Italy; the Ministry of Development of Turkey under Contract No. DPT2006K-120470; the National Science and Technology fund; the Olle Engkvist Foundation under Contract No. 200-0605; STFC (United Kingdom); the Knut and Alice Wallenberg Foundation (Sweden) under Contract No. 2016.0157; the Royal Society, United Kingdom under Contracts No. DH140054, and No. DH160214; the Swedish Research Council; and the U.S. Department of Energy under Contracts No. DE-FG02-05ER41374 and No. DE-SC-0012069.

[1] B. Aubert *et al.* (*BABAR* Collaboration), Phys. Rev. D **74**, 091103(R) (2006).
[2] B. Aubert *et al.* (*BABAR* Collaboration), Phys. Rev. D **76**, 012008 (2007).
[3] B. Aubert *et al.* (*BABAR* Collaboration), Phys. Rev. D **77**, 092002 (2008).
[4] J. P. Lees *et al.* (*BABAR* Collaboration), Phys. Rev. D **86**, 012008 (2012).

[5] M. Ablikim *et al.* (BES Collaboration), Phys. Rev. Lett. **100**, 102003 (2008).
[6] C. P. Shen *et al.* (Belle Collaboration), Phys. Rev. D **80**, 031101(R) (2009).
[7] M. Ablikim *et al.* (BESIII Collaboration), Phys. Rev. D **91**, 052017 (2015).
[8] M. Ablikim *et al.* (BESIII Collaboration), Phys. Rev. D **99**, 032001 (2019).
[9] M. Ablikim *et al.* (BESIII Collaboration), Phys. Rev. D **100**, 032009 (2019).
[10] M. Ablikim *et al.* (BESIII Collaboration), Phys. Rev. Lett. **124**, 112001 (2020).
[11] M. Ablikim *et al.* (BESIII Collaboration), Phys. Rev. D **102**, 012008 (2020).
[12] M. Ablikim *et al.* (BESIII Collaboration), Phys. Lett. B **813**, 136059 (2021).
[13] M. Ablikim *et al.* (BESIII Collaboration), arXiv:2105.13597
[14] P. R. Page, E. S. Swanson, and A. P. Szczepaniak, Phys. Rev. D **59**, 034016 (1999).
[15] G. J. Ding and M. L. Yan, Phys. Lett. B **650**, 390 (2007).
[16] J. Ho, R. Berg, T. G. Steele, W. Chen, and D. Harnett, Phys. Rev. D **100**, 034012 (2019).
[17] Y. H. Ma, Y. Chen, M. Gong, and Z. F. Liu, Chin. Phys. C **45**, 013112 (2021).
[18] G. J. Ding and M. L. Yan, Phys. Lett. B **657**, 49 (2007).
[19] X. Wang, Z. F. Sun, D. Y. Chen, X. Liu, and T. Matsuki, Phys. Rev. D **85**, 074024 (2012).
[20] C. G. Zhao, G. Y. Wang, G. N. Li, E. Wang, and D. M. Li, Phys. Rev. D **99**, 114014 (2019).
[21] Q. Li, L. C. Gui, M. S. Liu, Q. F. Lü, and X. H. Zhong, Chin. Phys. C **45**, 023116 (2021).
[22] T. Barnes, N. Black, and P. R. Page, Phys. Rev. D **68**, 054014 (2003).
[23] C. Q. Pang, Phys. Rev. D **99**, 074015 (2019).
[24] Z. G. Wang, Nucl. Phys. **A791**, 106 (2007).
[25] H. X. Chen, X. Liu, A. Hosaka, and S. L. Zhu, Phys. Rev. D **78**, 034012 (2008).
[26] N. V. Drenska, R. Faccini, and A. D. Polosa, Phys. Lett. B **669**, 160 (2008).
[27] C. R. Deng, J. L. Ping, F. Wang, and T. Goldman, Phys. Rev. D **82**, 074001 (2010).
[28] H. X. Chen, C. P. Shen, and S. L. Zhu, Phys. Rev. D **98**, 014011 (2018).
[29] H. W. Ke and X. Q. Li, Phys. Rev. D **99**, 036014 (2019).
[30] S. S. Agaev, K. Azizi, and H. Sundu, Phys. Rev. D **101**, 074012 (2020).
[31] R. R. Dong, N. Su, H. X. Chen, E. L. Cui, and Z. Y. Zhou, Eur. Phys. J. C **80**, 749 (2020).
[32] F. X. Liu, M. S. Liu, X. H. Zhong, and Q. Zhao, Phys. Rev. D **103**, 016016 (2021).
[33] C. F. Qiao, Phys. Lett. B **639**, 263 (2006).
[34] E. Klempt and A. Zaitsev, Phys. Rep. **454**, 1 (2007).
[35] L. Zhao, N. Li, S. L. Zhu, and B. S. Zou, Phys. Rev. D **87**, 054034 (2013).
[36] Y. B. Dong, A. Faessler, T. Gutsche, Q. F. Lü, and V. E. Lyubovitskij, Phys. Rev. D **96**, 074027 (2017).
[37] X. Cao, J. P. Dai, and Y. P. Xie, Phys. Rev. D **98**, 094006 (2018).
[38] Y. L. Yang, D. Y. Chen, and Z. Lu, Phys. Rev. D **100**, 073007 (2019).
[39] A. M. Torres, K. P. Khemchandani, L. S. Geng, M. Napsuciale, and E. Oset, Phys. Rev. D **78**, 074031 (2008).
[40] L. Alvarez-Ruso, J. A. Oller, and J. M. Alarcón, Phys. Rev. D **80**, 054011 (2009).
[41] B. B. Malabarba, X. L. Ren, K. P. Khemchandani, and A. M. Torres, Phys. Rev. D **103**, 016018 (2021).
[42] S. L. Zhu, Int. J. Mod. Phys. E **17**, 283 (2008).
[43] D. Y. Chen, J. Liu, and J. He, Phys. Rev. D **101**, 074045 (2020).
[44] V. P. Druzhinin, S. I. Eidelman, S. I. Serednyakov, and E. P. Solodov, Rev. Mod. Phys. **83**, 1545 (2011).
[45] B. Aubert *et al.* (*BABAR* Collaboration), Phys. Rev. D **76**, 092005 (2007).
[46] D. Y. Chen, J. Liu, and J. He, Phys. Rev. D **101**, 074045 (2020).
[47] M. Ablikim *et al.* (BESIII Collaboration), Chin. Phys. C **44**, 040001 (2020).
[48] C. H. Yu *et al.*, in *Proc. IPAC2016, Busan, Korea* (2016), https://doi.org/10.18429/JACoW-IPAC2016-TUYA01.
[49] S. Agostinelli *et al.* (GEANT4 Collaboration), Nucl. Instrum. Methods Phys. Res., Sect. A **506**, 250 (2003).
[50] R. G. Ping *et al.*, Chin. Phys. C **40**, 113002 (2016).
[51] P. A. Zyla *et al.* (Particle Data Group), Prog. Theor. Exp. Phys. **2020**, 083C01 (2020).
[52] A. Ryd *et al.*, EvtGen: A Monte Carlo generator for B-physics, EVTGEN-V00-11-07 (2005), https://inspirehep.net/literature/707695.
[53] M. Ablikim *et al.* (BESIII Collaboration), Chin. Phys. C **41**, 063001 (2017); **41**, 113001 (2017).
[54] M. Ablikim *et al.* (BESIII Collaboration), Phys. Rev. D **99**, 011101(R) (2019).
[55] M. Ablikim *et al.* (BESIII Collaboration), Phys. Rev. D **87**, 012002 (2013).
[56] H. Albrecht *et al.* (ARGUS Collaboration), Phys. Lett. B **340**, 217 (1994).
[57] R. G. Ping, Chin. Phys. C **38**, 083001 (2014).
[58] M. Ablikim *et al.* (BESIII Collaboration), Phys. Rev. D **103**, 072007 (2021).